Anal. Chem. **2007,** *79,* 3940−3944

Correspondence

Flow Photolysis for Spatiotemporal Stimulation of Single Cells

Carsten Beta,[†] Danica Wyatt,[†,‡] Wouter-Jan Rappel,[§] and Eberhard Bodenschatz*[,†,‡]

Max Planck Institute for Dynamics and Self-Organization, 37077 Göttingen, Germany, Laboratory of Atomic and Solid State Physics, Cornell University, Ithaca, New York 14853, and Center for Theoretical Biological Physics and Department of Physics, University of California, San Diego, La Jolla, California 92093

Quantitative studies of cellular systems require experimental techniques that can expose single cells to well-controlled chemical stimuli with high spatiotemporal resolution. Here, we combine microfluidic techniques with the photochemical release of caged signaling molecules to generate tailored stimuli on the length scale of individual cells with subsecond switching times. We exemplify this flexible approach by initiating membrane translocation of fluorescent fusion proteins in chemotactic *Dictyostelium discoideum* cells.

The response of cells to extracellular signals is ubiquitous in nature. Chemotaxis, the directed movement of a cell toward a chemical stimulus, is a prime example of a cell's reaction to complex external signals. It is essential to biomedical processes ranging from tumor metastasis[1] to immune reactions[2] and the development of the nervous system.[3] Over the past decade, understanding of the biochemistry behind directional sensing has seen a rapid advance through the use of fluorescent fusion proteins.[4] Many molecular players of the chemotactic signaling pathway could be indentified.[5] However, a mechanistic understanding of directional sensing in eukaryotic cells is largely missing. It requires quantitative data that characterize the response of chemotactic cells to well-defined external stimuli. The initial steps of the chemotactic signaling cascade take place within only a few seconds,[6] and time scales for the dynamics of the actin cytoskeleton were found to be even shorter.[7] Further progress in this field thus relies on experimental techniques that provide quantitative control of chemical stimuli on the length scales of individual cells, with a temporal resolution higher than the time scales of intracellular signaling events.

In traditional chemotaxis assays like the Boyden,[8] Zigmond,[9] or Dunn chambers,[10] gradient signals are established by diffusion through a porous medium or a narrow gap between two reservoirs of different concentration. Over the past decade, microfluidic techniques have been successfully established to generate well-controlled stimuli for single-cell experiments.[11] Stable concentration profiles can be generated ranging from linear[12] to more complex, periodic gradients[13] as well as exponential and parabolic profiles.[14] High spatial control is achieved in most of these devices. However, similar to classical gradient chambers, transient times for buildup and switching of gradient profiles are on the order of minutes, i.e., slower than the time scales of many intracellular signaling processes. Recently, attempts have been made to generate dynamically changing gradient signals in microfluidic chambers.[15] A switching time of ∼5 s could be achieved in a device that combines microstructured membranes with two microfluidic gradient generators.[16]

Here, we present an experimental method to stimulate single cells with high resolution in both space and time. In particular, our approach allows us to reduce transient times for the buildup of gradient profiles to below 1 s. It is based on the light-induced release of caged signaling substances in a microfluidic flow chamber. Through the interplay of fluid flow and light source geometry, a wide variety of concentration profiles can be generated. As an example for the application of this method, we initiate intracellular protein translocation in chemotactic cells of the

* To whom correspondence should be addressed. E-mail: eberhard.bodenschatz@ds.mpg.de. Tel.: +49 551 5176 300. Fax.: +49 551 5176 302.

† Max Planck Institute for Dynamics and Self-Organization.

‡ Cornell University.

§ University of California, San Diego.

(1) Condeelis, J.; Segall, J. E. *Nat. Rev. Cancer* **2003**, *3*, 921−930.
(2) Negulescu, P. A.; Krasieva, T. B.; Khan, A.; Kerschbaum, H. H.; Cahalan, M. D. *Immunity* **1996**, *4*, 421−430.
(3) Orourke, N. A.; Dailey, M. E.; Smith, S. J.; McConnell, S. K. *Science* **1992**, *258*, 299−302.
(4) Parent, C. A.; Blacklock, B. J.; Froehlich, W. M.; Murphy, D. B.; Devreotes, P. N. *Cell* **1998**, *95*, 81−91.
(5) Manahan, C. L.; Iglesias, P. A.; Long, Y.; Devreotes, P. N. *Annu. Rev. Cell Dev. Biol.* **2004**, *20*, 223−253.
(6) Parent, C. A.; Devreotes, P. N. *Science* **1999**, *284*, 765−770.
(7) Diez, S.; Gerisch, G.; Anderson, K.; Muller-Taubenberger, A.; Bretschneider, T. *Proc. Natl. Acad. Sci. U.S.A.* **2005**, *102*, 7601−7606.
(8) Boyden, S. *J. Exp. Med.* **1962**, *115*, 453−466.
(9) Zigmond, S. H. *J. Cell Biol.* **1977**, *75*, 606−616.
(10) Zicha, D.; Dunn, G. A.; Brown, A. F. *J. Cell Sci.* **1991**, *99*, 769−775.
(11) Breslauer, D. N.; Lee, P. J.; Lee, L. P. *Mol. Biosyst.* **2006**, *2*, 97−112.
(12) Jeon, N. L.; Dertinger, S. K. W.; Chiu, D. T.; Choi, I. S.; Stroock, A. D.; Whitesides, G. M. *Langmuir* **2000**, *16*, 8311−8316.
(13) Dertinger, S. K. W.; Chiu, D. T.; Jeon, N. L.; Whitesides, G. M. *Anal. Chem.* **2001**, *73*, 1240−1246.
(14) Irimia, D.; Geba, D. A.; Toner, M. *Anal. Chem.* **2006**, *78*, 3472−3477.
(15) Lin, F.; Saadi, W.; Rhee, S. W.; Wang, S. J.; Mittal, S.; Jeon, N. L. *Lab Chip* **2004**, *4*, 164−167.
(16) Irimia, D.; Liu, S. Y.; Tharp, W. G.; Samadani, A.; Toner, M.; Poznansky, M. C. *Lab Chip* **2006**, *6*, 191−198.

10.1021/ac070033y CCC: $37.00
Published on Web 04/14/2007

eukaryotic microorganism *Dictyostelium discoideum* by stimulation with cyclic adenosine 3′,5′-monophosphate (cAMP).

EXPERIMENTAL SECTION

Microfluidic Devices. Microfluidic channels of width $x = 500 \pm 0.5$ μm, length $y = 3000 \pm 0.5$ μm, and height $z = 25 \pm 0.5$ μm were produced by standard soft lithography techniques. This involved photolithographic patterning of a photoresist (SU-8 50, Micro Resist Technology) coated Si wafer (Wafer World Inc.), to generate a "master" wafer that carried a relief of the desired microstructure. Channels were produced by molding premixed poly(dimethylsiloxane) (PDMS; Sylgard 184, Dow Corning) against the master wafer. Inlets and outlets were punched through the PDMS using a sharpened syringe tip (19 gauge × 1 in., McMaster), and the channels were sealed with a glass coverslip (24 × 60 mm, No. 1, Gerhard Menzel Glasbearbeitungswerk GmbH & Co. KG) after a 2-min treatment in air plasma (PDC-002, Harrick Plasma). See the recent literature[12,17] for more details on soft lithography.

Cell Culture. We used cells of the eukaryotic microorganism *D. discoideum*. Experiments were performed with the AX3-derived strain WF38 that expressed a green fluorescent protein (GFP) fused to the PH domain of the cytosolic regulator of adenylyl cyclase (CRAC). Cells were grown in Petri dishes under HL5 medium (7 g/L yeast extract, 14 g/L peptone, 0.5 g/L KH_2PO_4, 0.5 g/L Na_2HPO_4). To establish chemotactic behavior,[18] cells were washed with phosphate buffer (2 g/L KH_2PO_4, 0.36 g/L $Na_2HPO_4 \cdot 2H_2O$, pH 6.0) and starved for 7−8 h in a Petri dish under a thin phosphate buffer film. Prior to the experiment, the cells were resuspended from the bottom of the Petri dish. The suspension was infused into the microfluidic channel, and cells were allowed to attach to the bottom glass plate of the channel for 5−10 min.

Solution Delivery. Teflon tubing (39241, Novodirect GmbH) was used to connect the microfluidic device to a syringe pump (PHD 2000, Harvard Apparatus Inc.), which operated a 500-μL gastight glass syringe (1750 TTLX, Hamilton Bonaduz AG) to maintain a constant flow of phosphate buffer through the channel. The flow velocity was 111 ± 2 μm/s unless stated otherwise. Concentration profiles were visualized by adding 10 μM (unless stated otherwise) of 4,5-dimethoxy-2-nitrobenzyl (DMNB)-caged fluorescein (dextran conjugate, 3000 MW, Invitrogen Corp.) to the flow. For stimulation of the *Dictyostelium* cells, 10 μM DMNB-caged cAMP (Invitrogen Corp.) was added instead. The concentration of photochemically released cAMP was quantified by comparison with DMNB-caged fluorescein.

Fluorescence Microscopy and Photoactivation. Imaging was performed with an inverted confocal laser scanning microscope (Fluoview FV1000, Olympus Corp.). It was equipped with an additional scanning unit to move a 405-nm laser (25 mW, FV5-LD405, Olympus Corp.) independent of the imaging lasers inside the field of view. Before the experiment, a microfluidic channel with starvation-developed cells was mounted on the microscope with the coverslip toward the objective. Photoactivation was initiated by rapidly scanning the 405-nm laser over a region in the flow upstream of a cell as indicated in Figure 1a.

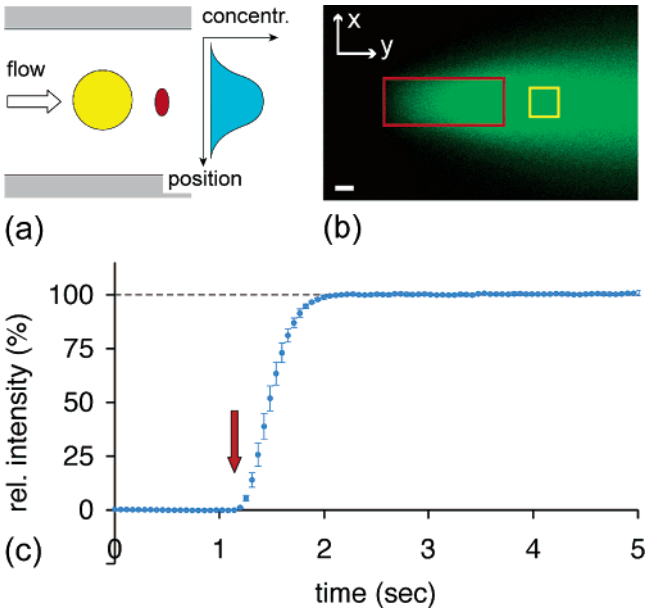

Figure 1. Uniform photoactivation experiment. (a) Schematic top view; the caged chemical is released inside an uncaging region of arbitrary shape (yellow) to produce the desired concentration profile (blue), which is carried across the cell (red) by the flow. (b) Release of 10 μM DMNB-caged fluorescein inside a rectangular uncaging region (red); steady state, measured at $z = 2$ μm; scale bar, 10 μm. (c) Fluorescence intensity averaged inside the yellow area indicated in (b), uncaging was initiated at $t = 1.14$ s (red arrow); the average over measurements at heights $z = 0$, 1, 2, 5, 7, and 10 μm is shown, the error bars indicating the standard deviation. Scanning speed of uncaging laser, 0.1 s/frame.

RESULTS AND DISCUSSION

A generic flow photolysis experiment for single-cell stimulation is displayed in Figure 1a. Cells are placed in a microfluidic channel under a continuous fluid flow that carries the caged, i.e., inert form of a signaling agent. The latter can be activated by photochemically splitting off the cage through exposure to short-wavelength irradiation. By illuminating a region in the flow immediately upstream of the cell, the uncaged signaling substance is carried across the cell by the fluid flow. To generate concentration profiles of arbitrary shape, the intensity of the uncaging light source needs to be sufficiently small, so that only a fraction of the molecules are uncaged when passing through the illuminated area. In this case, the transit time of a fluid element carried by the flow through the area of photoactivation determines the concentration of the released chemical. The shape of the uncaging region is thus linearly mapped onto the downstream concentration profile. The detailed spatial distribution of the uncaged chemical is determined by (1) the concentration of the caged compound in the flow, (2) its uncaging kinetics, (3) the diffusion constant of the uncaged compound, (4) the size and shape of the illuminated region, (5) the intensity of the uncaging light source, and (6) the flow speed.

We discuss each of these effects in the following. (1) For cell stimulation experiments, a fixed concentration of 10 μM DMNB-caged cAMP is used. (2) The uncaging process is quantified by comparison with the photochemical release of fluorescent dye from a 10 μM solution of DMNB-caged fluorescein. We choose a dye that carries the same caging group as the signaling agent, so

(17) Whitesides, G. M.; Ostuni, E.; Takayama, S.; Jiang, X. Y.; Ingber, D. E. *Annu. Rev. Biomed. Eng.* **2001**, *3*, 335−373.
(18) Chisholm, R. L.; Firtel, R. A. *Nat. Rev.* **2004**, *5*, 531−541.

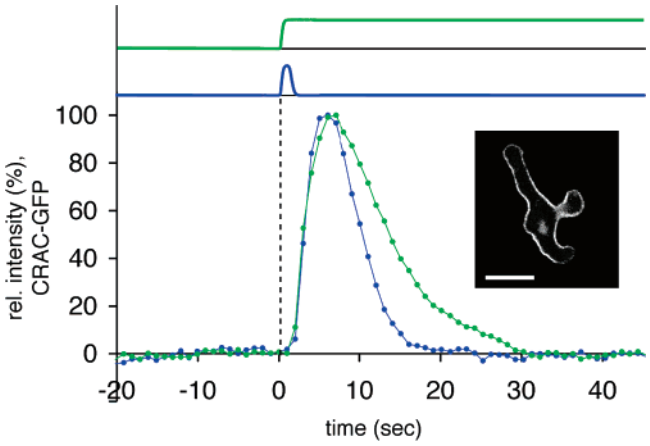

Figure 2. Translocation of CRAC-GFP in chemotactic *Dictyostelium* cells. (top) Temporal evolution of a continuous (green) and a short (blue) stimulus generated by uncaging 10 μM DMNB-caged cAMP, peak levels correspond to a concentration of 10 μM, determined by comparison with DMNB-caged fluorescein. (bottom) CRAC-GFP response of chemotactic *Dictyostelium* cells to the continuous (green) and short (blue) stimuli shown above. The normalized ratio between the fluorescence intensity at the membrane (averaged inside a 1.2-μm-wide zone at the membrane) and in the cytoplasm is shown, averaged over 11 (green) and 10 (blue) cells, respectively. (inset) Example of global translocation of CRAC-GFP in a *Dictyostelium* cell; scale bar, 10 μm.

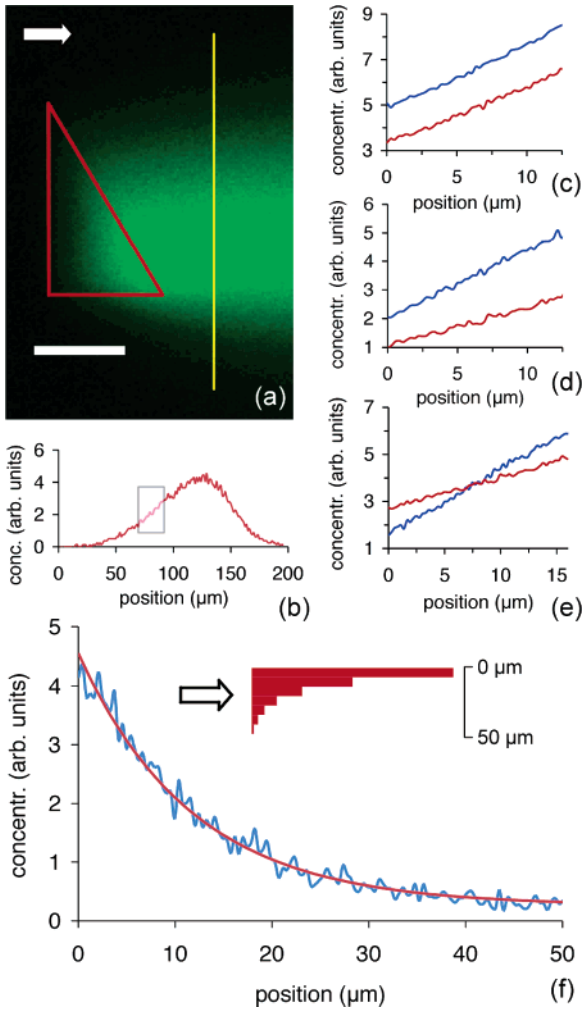

Figure 3. Directional photoactivation experiment I. (a) Photorelease of 5 μM DMNB-caged fluorescein in a triangular uncaging region (red); scale bar, 50 μm; arrow, direction of flow. (b) Fluorescence intensity along the yellow line in (a) for a mean flow speed of 67 μm/s. (c) to (e) Zoom of shaded region in (b) for different gradients, (c) constant slope and different midpoint, (d) constant relative gradient, and (e) different slope and constant midpoint. The different gradients were generated by (c) changing the background concentration of fluorescein by +1.25 μM, (d) changing the intensity of the uncaging laser by a factor of 0.61, and (e) increasing the background fluorescein concentration by +2.5 μM and changing the intensity of the uncaging laser by a factor of 0.55. (f) Nonlinear gradient profile (blue) with exponential fit $0.26 + 4.3e^{-0.085x}$ (red). (f, inset) Shape of the uncaging region (red), the concentration profile is measured along the black line from 0 to 50 μm; arrow, direction of flow; flow speed, 1110 μm/s.

that similar uncaging kinetics can be expected. The amount of released dye is measured by comparison with the fluorescence from a solution in which all dye has been uncaged. (3) If the flow speed becomes small compared to the time scale of diffusive transport, the distribution of the uncaged component is influenced by diffusion perpendicular to the flow. For the diffusion constants of nucleotides in aqueous solution, values around 400 $\mu m^2/s$ have been reported.[19] This is sufficiently close to the value of 260 $\mu m^2/s$ for the dextran-conjugated fluorescein used here,[20] so that diffusive broadening of the cAMP concentration profiles will be comparable to the distribution observed with uncaged fluorescein. (4) The shape of the photoactivation area that is scanned by the uncaging laser can be tuned to control the spatial distribution of uncaged chemical at the location of the cell. The wider the illuminated region extends in the direction of the flow, the longer the caged substance spends under the light source and the more of the signaling agent will be released. (5) The intensity of the uncaging laser can be tuned between 0 and 100%. For the experiments presented in the following, we have used full laser power in all cases. Note that the effective intensity depends on the size of the illuminated region, since the laser needs a longer time to scan a larger area. (6) The exposure of a fluid element to the uncaging light source is furthermore controlled by the flow speed. For increasing speed, the exposure time is reduced, so that less of the caged substance is released. To ensure temporal stability of the concentration profile, the flow speeds were chosen such that the uncaging laser scans the region of photoactivation at least five times during the average period of time a fluid element spends inside this region.

Through the interplay of these effects, a wide range of concentration profiles can be tailored. These profiles can be applied with a high temporal resolution by turning the uncaging laser on and off in the course of time. The time scales for buildup of a desired concentration distribution are ultimately limited by Taylor dispersion.[21] In our setup, the photochemically released substance is carried only over a short distance by the flow before reaching the cell, so that broadening of a concentration front due to Taylor dispersion is kept at a minimum. Transient times for buildup of a stationary profile are thus determined by the time a fluid element spends unter the uncaging light source. With a flow

(19) Bowen, W. J.; Martin, H. L. *Arch. Biochem. Biophys.* **1964**, *107*, 30−36.
(20) Bae, A. MPIDS, Göttingen, Germany, personal communication. 2006,
(21) Stone, H. A.; Stroock, A. D.; Ajdari, A. *Annu. Rev. Fluid Mech.* **2004**, *36*, 381−411.

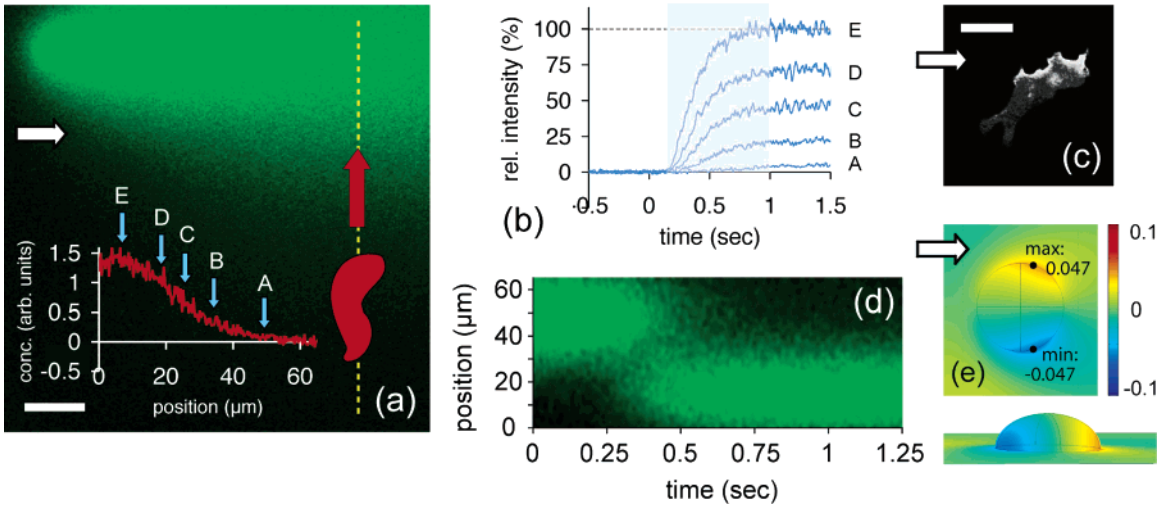

Figure 4. Directional photoactivation experiment II. (a) Photorelease of 10 μM DMNB-caged fluorescein by a laser point source of 2.6 μm in diameter located in the upper left corner; scale bar, 10 μm; flow from left to right. (a, inset) Fluorescence intensity along the dashed yellow line. (b) Temporal buildup of gradient profile, initiated at time 0 s, measured at different locations in the profile shown in the inset of (a). (c) Directional translocation of CRAC-GFP in a chemotactic *Dictyostelium* cell exposed to a gradient of cAMP generated as in (a); scale bar, 10 μm. (d) Gradient reversal: Space−time diagram perpendicular to the flow downstream of the laser point source. At time 0 s, the laser was moved from the upper to the lower half of the domain. (e) Numerical finite element simulation of a cell (height of 5 μm, circular bottom of radius 7.5 μm) in a linear concentration gradient (the imposed concentration changes by 30% across the length of the cell) inside a microfluidic channel (flow speed and channel dimensions as in the experiment), performed using the software package FEMlab. Concentration increases from bottom to top, fluid flow from left to right. The deviations in concentration from the imposed linear profile stay within 10%, from ref 26.

speed higher than 100 μm/s and a region of photouncaging that extends less than 100 μm in the direction of the flow, subsecond switching times can be readily achieved.

In the following, we show examples to demonstrate the temporal and spatial flexibility of our method. We can generate rapidly switching, spatially uniform signals by scanning a rectangular region with the uncaging laser. Figure 1b shows uncaging of 10 μM DMNB-caged fluorescein after a steady state has been reached. Extending the rectangular uncaging region in the direction of the flow did not increase the fluorescence intensity further, indicating that all caged fluorescein was released. Upon initiation of photouncaging, a rise in concentration was observed downstream of the uncaging light source. In Figure 1c, the temporal evolution of the intensity is displayed as recorded inside the yellow area indicated in Figure 1b. Switching was completed after 0.8 s. We have performed confocal scans at different heights above the bottom glass plate of the channel and found that the switching speed varied by less than 0.07 s over the entire height of the channel. Figure 1c shows the switching event averaged over different *z*-planes.

We exemplified our approach by inducing intracellular protein translocation in cells of the eukaryote *D. discoideum*, a well-established model organism for the study of cell motility and chemotaxis.[22] Proteins containing the pleckstrin homology (PH) domain are known to translocate from the cytosol to the plasma membrane upon external stimulation with cAMP.[4] Starvation-developed *D. discoideum* cells were placed in a microfluidic channel as described in the Experimental Section. Throughout the experiment, they were kept under a gentle flow of phosphate buffer containing 10 μM DMNB-caged cAMP. The cells were affected neither by the weak shear flow[23] nor by the caged cAMP, as was verified by independent micropipet experiments. The cells showed no measurable response to the caged cAMP until the caging group was photochemically split off.

We studied PH domain localization in chemotactic *Dictyostelium* cells stimulated by a uniform level of cAMP. Upon exposure to a short 1 ± 0.1 s pulse of 10 μM cAMP, translocation of CRAC-GFP to the plasma membrane was observed. The membrane-bound signal peaked 6 s after initiation of the pulse and then rapidly decayed to reach its initial level after ~20 s; see Figure 2. Upon continuous stimulation with 10 μM cAMP, a strikingly similar translocation event was observed, demonstrating the efficient mechanisms of adaptation of *Dictyostelium* cells to high levels of cAMP. However, a slower decay of the membrane-bound signal was found in the case of a continuous stimulus.

The creation of a localized linear gradient by a triangular uncaging region is demonstrated in Figure 3a. The concentration profile of uncaged fluorescein downstream of the uncaging region is shown in Figure 3b, measured along the yellow line in (a). A widening due to diffusion can be observed at the edges. In the middle, however, a linear regime can be clearly distinguished, marked by a gray-shaded region in (b). In Figure 3c, d, and e, we show examples of how our setup can be used to systematically produce different linear gradients inside this area. Gradients of constant slope Δc and different midpoint c_0 are obtained by changing the background concentration of fluorescein; see Figure 3c. Constant relative gradients $\Delta c/c_0$, Figure 3d, can be generated by changing the intensity of the uncaging laser. Finally, profiles of different slopes and constant midpoint require a change in both the background concentration and the intensity of the uncaging

(22) Van Haastert, P. J. M.; Devreotes, P. N. *Nat. Rev. Mol. Cell Biol.* **2004**, *5*, 626−634.

(23) Song, L.; Nadkarni, S. M.; Bödeker, H. U.; Beta, C.; Bae, A.; Franck, C.; Rappel, W.-J.; Loomis, W. F.; Bodenschatz, E. *Eur. J. Cell Biol.* **2006**, *85*, 981−989.

light source, Figure 3e. See the caption of Figure 3 for the parameters of these specific examples.

Besides linear gradients, nonlinear profiles can also be created by tuning the shape of the trianglar uncaging area. As an example, a concentration profile is shown in Figure 3f together with the corresponding exponential fit. In this case, the illuminated region is composed of a sequence of bars; see inset of Figure 3f. Their different extensions in the direction of the flow are determined by an exponential relation.

In cases where no specific gradient profile is required, directional signals can be produced by a point source. The uncaged signaling substance is carried downstream of the light spot and, at the same time, spreads perpendicular to the direction of the flow due to diffusion. A stationary concentration profile of Gaussian shape is created, with a width that is controlled by the flow speed and the distance from the light source in the direction of the flow; see Figure 4a. In Figure 4b, the buildup of a gradient profile is shown in the course of time. The uncaging laser is switched on at $t = 0$ s, followed by a rise in concentration, shown for different locations in the gradient profile, as indicated in the inset of Figure 4a. Similar to uniform signals, a switching time of ~0.8 s can be achieved for establishing the gradient profile. In Figure 4c, directional translocation of CRAC-GFP in a chemotactic *Dictyostelium* cell is shown in response to a gradient stimulus generated as in Figure 4a. More complex protocols of spatiotemporal stimulation can be readily implemented with this method. For example, the direction of the gradient signal can be switched in less than 1 s by changing the position of the uncaging light source. In Figure 4d, this is demonstrated in a space−time diagram that was recorded perpendicular to the flow immediately downstream of the laser point source. At $t = 0$ s, the laser is moved from a position in the upper half of the domain down to a position at around $x = 17$ μm. The space−time diagram shows that the new concentration profile is established after ~750 ms.

Our approach is restricted to signaling substances that are available in a photochemically caged form. However, much progress has been made in recent years in the preparation and handling of caged compounds.[24] A large variety of photoactivatable chemicals are available commercially, and detailed protocols are at hand for custom-made synthesis of less commonly used substances. In previous work, photouncaging has been used to stimulate cells in the absence of fluid flow.[25] In this case, the gradient profile is not stationary in time and its shape is difficult to control, similar to micropipet experiments. In addition, in these cases, the laser uncaged substance, as well as signaling agents and waste products released by the cells themselves, are not removed. In the microfluidic chamber used here, the flow immediately washes away all of these substances and thus prevents the buildup of an uncontrolled chemical background. Compared to a perfusion chamber, a microfluidic channel has the advantage that only small amounts of fluid are needed and the properties of the fluid flow can be controlled with high precision. In general, however, our method can be used in any closed or open perfusion system. Furthermore, the idea of flow photolysis is not limited to a confocal laser scanning setup but can be readily implemented in simpler microscopy systems.

We have demonstrated that the combined use of photouncaging and fluid flow provides temporal stability and quantitative control of gradient profiles. Note that the interplay of cell geometry, flow speed, and diffusion can influence the concentration profile in the vicinity of the cell. We have performed numerical finite element simulations to characterize the three-dimensional flow problem.[26] In our case, the concentration on the cell surface was found to deviate from the imposed gradient profile by less than 10%; see Figure 4e.

In conclusion, we have introduced a versatile approach to perform well-controlled single-cell experiments combining microfluidic tools with photoactivation of caged signaling substances. We expect this technique to contribute to our quest for a quantitative understanding of intracellular signaling.

ACKNOWLEDGMENT

We thank William F. Loomis for suggesting the use of caged cAMP and for useful discussions. This work was supported by the Max Planck Society and the NSF-sponsored Center for Theoretical Biological Physics (W.-J.R.).

Received for review January 5, 2007. Accepted March 26, 2007.

AC070033Y

(24) Marriott, G.; Roy, P.; Jacobson, K. In *Biophotonics, Part A*; Marriott, G., Parker, I., Eds.; Academic Press Inc: San Diego, 2003; Vol. 360, pp 274−288.

(25) Samadani, A.; Mettetal, J.; van Oudenaarden, A. *Proc. Natl. Acad. Sci. U.S.A.* **2006**, *103*, 11549−11554.

(26) Fröhlich, T.; Bodenschatz, E.; Beta, C. In preparation.